Thermoluminescence Studies of Defect Trapped Charges in CeO$_2$ Nanoparticles

B. Soni, S. Biswas*

*Department of Physics, The LNM Institute of Information Technology, Jaipur-302031, India.

Abstract

Here, we report thermoluminescence (TL) studies of pristine CeO$_2$ nanoparticles synthesized via a sol-gel type chemical precursor method. The fluorite type crystal structure in the derived CeO$_2$ nanoparticles was confirmed with X-ray diffraction (XRD) studies. The average crystallite size calculated from XRD peak was 6 nm and 10 nm in the samples heat-treated at 400°C and 500°C, respectively. Rietveld refinement of the XRD data revealed the lattice parameter, a to be 0.5395 nm and 0.5392 nm, respectively in these two sets of samples. The shape and morphology of the nanoparticles were studied with scanning and high resolution tunnelling electron microscopes (SEM and HRTEM). The CeO$_2$ samples were exposed to ^{60}Co γ-radiation at room temperature for 1 h with a dose of 0.37 kGy/h and the TL glow curves were recorded at a heating rate of 5°K/s. The obtained TL glow curves were deconvoluted and Chen's method was followed to calculate the trapping parameters, viz. activation energy (E), order of kinetics (b), and frequency factor (s).

Keywords: *CeO$_2$ nanoparticles; Thermoluminescence; Chen's method; Defect states.*

PACS Code: *81.20.Ka; 78.60.Kn; 71.55.-i.*

1.0 INTRODUCTION

Thermoluminescence (TL) is the occurrence of thermally stimulated emission of light from a solid insulator or semiconductor that has been previously exposed to ionizing radiation such as α, β, or γ-rays under conditions of increasing temperature [1-3]. During irradiation, the excited electrons and holes from the valance bands are trapped in the localized energy levels within the forbidden gap created by impurities, luminescent centers and other imperfections present in the crystal. On heating, sufficient energy in the form of thermal vibrations causes the release of these trapped electrons which gives the characteristics of a thermoluminescent material. TL is one of the important techniques to study the physical parameters of traps in materials. The spatial and energy distribution of the charge carrier traps influence the optical properties of the luminescent materials. The qualitative information about the trap centers and trap parameters have favored the applications of this technique in various disciplines including geology, forensic science, solid state physics, and archeology.

Cerium oxide (CeO$_2$) is a rare-earth oxide with an optical band gap (~3eV at room temperature) and has been widely used in various applications including electrolytes in fuel cells, catalysis, oxygen sensing, luminescent materials, and UV-shielding [4-6]. In addition, it has also attracted interest in applications in glasses, ceramics, phosphors, and abrasives [7]. Chemically CeO$_2$ is highly stable and maintains its fluorite type (space group Fm3m) crystal structure up to its melting temperature ~ 2400 °C.

Here, we report our studies on defect trapped charges in CeO$_2$ nanoparticles derived by a sol-gel type chemical method.

2.0 EXPERIMENTALS

The synthesis technique involves a reaction between aqueous solution of cerium nitrate hexahydrate [Ce(NO$_3$)$_3$.6H$_2$O] and freshly prepared transparent *poly*-vinyl alcohol (PVA)-sucrose solutions at 70°C of reaction temperature with constant stirring. After the reaction, the transparent polymer solution turned yellowish in color. The highly viscous solution was aged at room temperature for 48 h. The derived gel was dried at 60-70°C and the obtained precursor powder was heat treated at 400-800°C in ambient air for selected time periods to develop the recrystallized CeO$_2$ nanoparticles.

364

* Corresponding author: Tel: +91 7597171575; Email: drsomnathbiswas@gmail.com

The crystalline structure of the derived samples was analyzed with XRD studies (RigakuMiniflex-2) using CuK_α radiation of 0.15406 nm. The morphology of the derived samples was studied with FESEM (Carl Zeiss SUPRA 55). Finer microstructural details of the samples were further analyzed with a JEM-2100 HRTEM. The TL glow curves were recorded using Nucleonix TL1009 spectrometer, consisting of a small metal plate heated directly using a temperature programmer, photomultiplier tube, dc amplifier and millivolt recorder. The samples (5 mg) were exposed to ^{60}Co γ-radiation at room temperature for 1 h with a dose of 0.37 kGy/h and the glow curves were recorded at a heating rate of 5°K/s. The recorded TL glow curves were deconvoluted and Chen's method was followed to calculate the trapping parameters, *viz.* activation energy (E), order of kinetics (b), and frequency factor (s).

3.0 RESULTS AND DISCUSSIONS

Figure 1 shows the XRD plots of the derived CeO_2 nanoparticles after heat treating in ambient air for 2 h at(a) 400°C and (b) 500°C, respectively. The plots confirm the highly crystalline nature of the derived ceria nanoparticles. The reflection peaks from (111), (200), (220), (311), (222), (400), (331), and (420) planes match well with the face-centered cubic ceria with Fm3m space group (JCPDS card 34-0394). No peaks of cerium nitrate or any other crystalline phase were obtained.
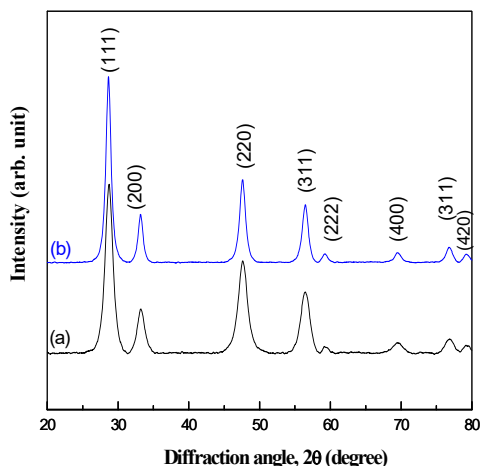
Fig. 1: XRD patterns of the derived CeO₂ nanoparticles after heat treating the precursor powders at (a) 400°C and (b) 500°C for 2 h in ambient air.

The average crystallite size calculated from the XRD peak widths using Scherrer's formula was 6 nm and 10 nm in the samples heat-treated at 400°C and 500°C, respectively. Rietveld refinement of the XRD data revealed the lattice parameter, *a* to be 0.5395 nm and 0.5392 nm in these two samples.

The FESEM image in Figure 2 reveals the morphology of the ceria nanoparticles heat treated at 400°C for 2h. The micrograph shows loosely agglomerated particles of spherical shape with typical size ranging between 10-20 nm. Figure 3 shows the typical HRTEM micrograph of the ceria nanoparticles heat treated at 400°C. As can be observed, the typical size of the particles is approximately 5 nm, which matches well with average crystallite size of 6 nm calculated from XRD data.
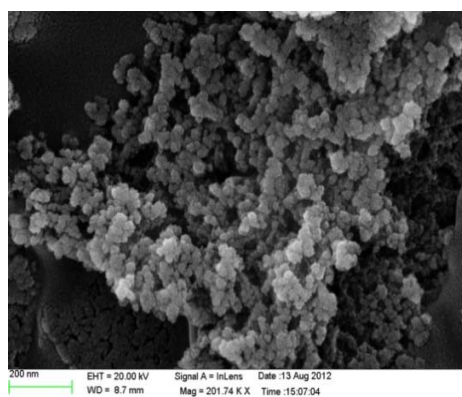
Fig. 2: FESEM image of the derived CeO₂ nanoparticles after heat treating the precursor powders at 400°C for 2 h in ambient air.
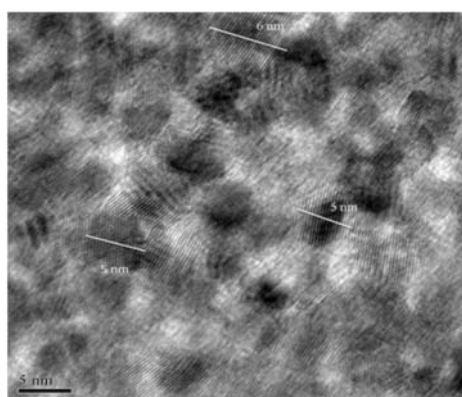
Fig. 3: HRTEM image of the CeO₂ nanoparticles derived after heat treating the precursor powders at 400°C for 2h in ambient air.

Figure 4 shows the TL glow-curve of CeO_2 nanoparticles heat treated at 500°C.
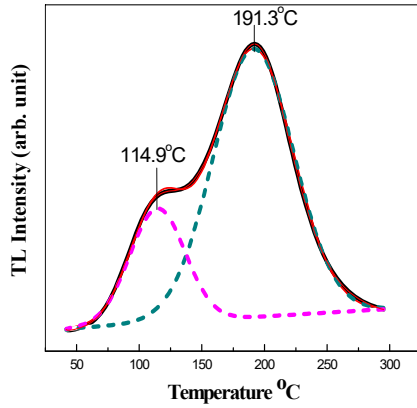
Fig. 4: TL glow curve of CeO$_2$ nanoparticles (heat treated at 500°C)at room temperature after exposing to ^{60}Co γ-radiation for 1 h.

In literature, different techniques were reported to determine the trapping parameters, *viz*, activation energy (*E*), order of kinetics (*b*), and frequency factor (*s*) [2,3]. In the present study, these parameters were calculated using Chen's half width method based on the shape of the glow curve [2].The deconvoluted curve in Figure 4 revealed two peaks positioned at 114.9°C and 191.3°C obeying 2nd order kinetics. To analyze the observed TL process, the shape parameters, $\delta = T_2 - T_m$, $\tau = T_m - T_1$, $\omega = T_2 - T_1$, Balarian parameter, $\gamma = \delta / \tau$ and symmetry factor, μ_g were calculated, where T$_m$ is peak temperature at maximum, T$_1$ and T$_2$ (T$_1$<T$_2$) are the temperature on either side of T$_m$ at half intensity. The values of $\mu_g$for peak 1 and peak 2 were calculated to be 0.50 and 0.51. The values of γ were calculated to be 1.02 and 1.03 for peak 1 and peak 2, respectively. As can be observed from the values of μ_g and γ, both the peaks correspond to 2nd order kinetics. The activation energy (*E*) was calculated using Chen's equation [2] :

$$E = c_\alpha \frac{kT_m^2}{\alpha} - b_\alpha(2kT_m) \qquad (1)$$

where, *k* is Boltzmann's constant and α stands for either τ, δ or ω, and can be expressed as,

$c_\tau = 1.51 + 3.0(\mu_g - 0.42)$ and

$b_\tau = 1.58 + 4.2(\mu_g - 0.42)$

$c_\delta = 0.976 + 7.3(\mu_g - 0.42)$ and $b_\delta = 0$

$c_\omega = 2.52 + 10.2(\mu_g - 0.42)$ and $b_\omega = 1$.

The frequency factors were calculated using the equation given by Chen and Winer [3],

$$\beta E/kT_m^2 = s\left[1 + \frac{\{(b-1)2kT_m\}}{E}\right]\exp\left(-\frac{E}{kT_m}\right), \qquad (2)$$

where β is the heating rate. The frequency factors (s) corresponding to peak 1 and peak 2 are 2.53 x 10^9 and 6.10 x 10^{7}s^{-1}, respectively. Table 1 summarizes the values of trapping parameters including symmetry factor and Balarian parameter as calculated from the TL glow curves of the CeO$_2$ nanoparticles (500°C heat treated) using Chen's half width method.

Table 1: Trapping parametersas obtained using Chen's peak shape method.

Sample (CeO$_2$)	T$_m$ (°C)	μ_g	Γ	b	*E* (eV)	s (s^{-1}) x 10^6
Peak 1	114.93	0.50	1.02	2	0.77	2530
Peak 2	191.25	0.51	1.03	2	0.78	61

A schematic representation of the band structure of CeO$_2$ is shown in Figure 5. The forbidden energy gap of CeO$_2$ is ~ 6 eV. However, the optical band gap is ~ 3.2 eV which is formed by empty 4f states of Ce^{4+} and is governed by charge transfer from O2p states to the empty 4f shell of Ce^{4+}.
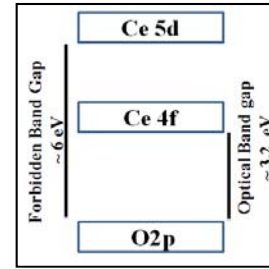
Fig. 5: Band structure of CeO$_2$.

In CeO$_2$, the luminescence is strongly dependent on its stoichiometry in the nanocrystals and is controlled by different F-centers (F^0, F$^+$, F^{2+}), subsurface defects, and also by the Ce^{3+}ions in non-stoichiometric ceria crystals [8]. The oxygen vacancies are the most prominent defects in nanocrystalline ceria. Nanocrystalline CeO$_2$ has a propensity to release more oxygen due to the high surface-to-volume ratio. Two electrons are left free from the oxygen atoms upon the formation of neutral oxygen vacancies. These free electrons are either localized near two Ce^{4+} ions neighboring the vacancy sites or are captured by intrinsic oxygen vacancies. These sites (known as F-centers) may act as trap centers for free electrons. The electronic level of these traps centers lies close to the bottom of empty 4f^0 band and hence may trap the electrons from 4f states [9].The localization of electronson the Ce^{4+}

ions results in the reduction of Ce^{4+} ions to Ce^{3+} ions and as a result 4f band is partial filled and splits into 4f full ($4f^1$) and 4f empty ($4f^0$) bands with $4f^1$ band getting placed close to the O2p valence band [10]. The 2nd order glow curve is generally observed if the probability of re-trapping is high [8]. Figure 6 shows the schematic representation of the possible trapping of the electrons by the trap centers in CeO_2 nanoparticles.
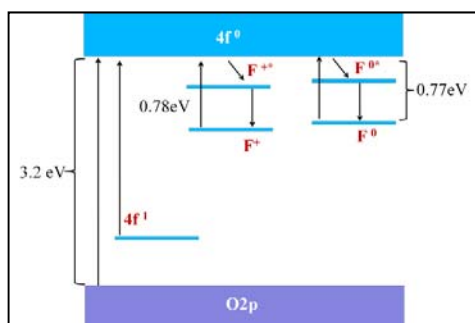
Fig. 6: Schematic representation of trapping phenomena in CeO₂nanoparticles.

The first peak observed in deconvoluted TL curve may be assigned to the phenomenon of de-trapping of electrons from the excited state (F^{0*}), since it is positioned near the bottom of the $4f^0$ state and again getting trapped into its ground state F^0 center. The second peak may be due to the electron getting de-trapped from the excited state (F^{+*}) center as it is positioned below F^{0*} center, and the electrons getting re-trapped into the ground state F^+ center.

4.0 CONCLUSION

Thermoluminescence studies of CeO_2 nanoparticles synthesized by a chemical precursor method revealed presence of two trap centers of 2nd order kinetics. The activation energy of the traps was evaluated to be 0.77 and 0.78 eV using Chen's half width method. For further analysis of the defect states in band gap and to identify oxygen vacancy defects in different charge states, photoluminescence studies will be performed that will provide further information on the band structure in the derived CeO_2 nanoparticles.

References

1. S. W. S. McKeever, Thermoluminescence of Solids, Cambridge University Press, 1983.
2. G. Kitis and V. Pagonis, Nuclear Instruments and Methods in Physics Research B 262 (2007) 313-322.
3. G. Kitis, R. Chen, and V. Pagonis, Physica status solidi (a) 205 (2008) 1181-1189.
4. S. Yabe, M. Yamashita, S. Momose, K. Tahira, S. Yoshida, R. Li, S. Yin, T. Sato, International Journal of Inorganic Materials, 3 (2001) 1003-1008.
5. H. Yang, C. Huang, A. Tang, X. Zhang, W. Yang, Materials Research Bulletin, 40 (2005) 1690-1695.
6. M. Nolan, J. E. Fearon, G. W. Watson, Solid State Ionics, 177 (2006) 3069-3074.
7. S. Basu, P. S. Devi, S. S. Maiti, Journal of Materials Research, 19 (2004) 3162-3171.
8. P. O Maksimchuk, V. V. Seminko, I. I. Bespalova, A. A. Masalov, Functional Materials, 21 (2014) 152-157.
9. A. Masalov, O. Viagin, P. Maksimchuk, V. Seminko, I. Bespalova, A. Aslanov, Y. Malyukin, and Y.Zorenko, Journal of Luminescence, 145 (2014) 61-64.
10. S. Askrabic, Z. D. Dohcevic, V. D. Araujo, G. Ionita, M. M. Lima, and A. Cantarero, Journal of Physics D: Applied Physics, 46 (2013) 495306.